Title
NUTATION SEQUENCES FOR MAGNETIC RESONANCE IMAGING IN SOLIDS

Author
Cho, H.M.

Publication Date
1985-07-01

Lawrence Berkeley Laboratory
UNIVERSITY OF CALIFORNIA

Materials & Molecular Research Division

Submitted to Physical Review Letters

NUTATION SEQUENCES FOR MAGNETIC RESONANCE IMAGING IN SOLIDS

H.M. Cho, C.J. Lee, D.N. Shykind,
and D.P. Weitekamp

July 1985

Prepared for the U.S. Department of Energy under Contract DE-AC03-76SF00098

DISCLAIMER

NUTATION SEQUENCES FOR MAGNETIC RESONANCE IMAGING IN SOLIDS

H. M. Cho, C. J. Lee, D. N. Shykind and D. P. Weitekamp

Department of Chemistry, University of California and Materials and Molecular Research Division, Lawrence Berkeley Laboratory, Berkeley CA 94720

Abstract

Novel radiofrequency nuclear magnetic resonance (NMR) pulse sequences are presented and their application to imaging of solids using rf field gradients is discussed. The sequences cause a nuclear spin to precess about the static field direction at a rate proportional to the strength of certain of the pulses. This forced precession is independent of the resonance offset and of couplings to other spins. The pulse sequence design is described using coherent averaging theory and is confirmed experimentally and numerically.

Imaging of the spatial distribution of nuclear spins by recording their magnetic resonance signals in field gradients is a well-known concept with a growing body of applications, particularly in medicine. The central idea is that the linear dependence of the frequency of spin precession on the magnetic field at the nucleus can be converted to a measurement of position along a known field gradient[1]. Practical implementation in two and three dimensions is accomplished by various time domain schemes which involve switching the direction of the gradient[2].

Nearly all NMR imaging has been done on liquids at resolutions of 10^{-3} - 10^{-1} cm, but the excellent chemical, orientational and motional specificity of NMR, as well as its noninvasive, penetrating nature, suggests that such imaging methods applicable to solids[3-10] would be valuable in materials science. The first barrier to NMR imaging encountered in solids is the broad and unresolved absorption spectrum caused by anisotropic spin interactions, which in liquids are averaged away by diffusive motions. In order to resolve two points in the spin distribution separated by a distance Δr and each having a spectral width $M_2^{1/2}$, a gradient of magnitude $G \gtrsim M_2^{1/2}/\Delta r$ is required. A typical value for protons in a solid would be $G \gtrsim 50$mT /cm ($M_2^{1/2}$ = 0.5 mT, $\Delta r = 10^{-2}$cm). Rapidly switching the amplitude and direction of a gradient of this size within the bore of a high field magnet is impractical. A time domain view of this inequality is that the precession in the field gradient must last long enough to create a significant difference in phase angle between the magnetization from adjacent picture elements, but that during this time the decay of the magnetization at each point should be minimal. Imaging has been demonstrated without meeting this condition[9], but only at the cost

of a large loss in signal energy. In applications this would lead to unacceptably long acquisition times and thus is not a general solution.

The principal contribution to $M_2^{1/2}$ for spin 1/2 nuclei in solids is the direct dipolar coupling to nearby spins. Three general approaches have been demonstrated previously which address this fact to achieve NMR imaging of solids with field gradients of less than a millitesla per centimeter. The first [3,4,10] is to use multiple pulse line narrowing techniques [11-16] or related modulation schemes[5] to effectively eliminate homonuclear dipolar couplings. The second [6] is to use the high-order multiple quantum spectra obtainable in solids to increase the line separation due to the applied gradient by a factor n equal to the number of Larmor frequency quanta characterizing the observed spectrum. The third[7] is to observe a dilute spin 1/2 isotope (^{13}C), whose spectrum is narrowed by heteronuclear decoupling of the neighboring protons.

The second largest contribution to the spectral width $M_2^{1/2}$ is the distribution of chemical shifts. This distribution is typically greater in solids than in fluids due to the extra contribution of the anisotropic part of the shift tensor. Since the chemical shift range increases linearly with magnetic field, it is a particularly severe impediment to imaging at a high Larmor frequency, which is otherwise desirable to maximize the signal-to-noise ratio. Two general approaches have been suggested for separating the distribution of chemical shifts from the spatial distribution of nuclear spins in solids. The simplest method[17] is to systematically vary the strength of the field gradient either within[7] or between[9,10] pulse sequences. This provides a data set from which the chemical shift and spatial distributions can be deconvolved. The price paid is a lower signal energy and a longer data acquisition time. This is

a poor bargain when the chemical shift distribution is unresolved due to powder broadening, chemical complexity, or poor field homogeneity as is typically the case for abundant spins in disordered solids. The second approach[4], which has not to our knowledge been experimentally demonstrated, combines multiple pulse line narrowing with pulsed DC field gradients in between the rf pulses. The phase of the rf and sign of the DC can be chosen in such a way that, over a cycle of several pulses, evolution due to the chemical shifts vanishes, but that due to the gradient accumulates. The gradient switching time of $\lesssim 10^{-6}$s required for this scheme is a significant barrier to its experimental implementation.

This Letter introduces a new approach to NMR imaging of nuclear spins in solids. Without the use of pulsed DC gradients or deconvolution, both dipolar (homonuclear and heteronuclear) and chemical shift contributions to $M_2^{1/2}$ are suppressed leaving only the spatial information. As in the proposal of Mansfield and Grannell[4] we begin with a cycle of rf $\pi/2$ pulses whose net effect is to eliminate any evolution of the transverse magnetization due to the rotating frame spin Hamiltonian. Two such cyclic sequences are shown in Fig. 1. The first (Fig. 1a) consists of sixteen Larmor frequency pulses alternating with delays or "windows" and has already appeared as part of a heteronuclear sequence in another context.[18] The second example (Fig. 1c) is of the windowless variety and differs from previous such sequences[19] in that it eliminates heteronuclear dipolar couplings and chemical shifts as well as homonuclear couplings. The result of Fourier transforming the cyclically sampled transverse magnetization obtained with these sequences is a single line at the spectrometer carrier frequency. This is the zero point of the rotating frame frequency scale. Such an experimental result on adamantane at a

proton Larmor frequency of 180 MHz is shown in Fig. 2a. The experimental width of 64 Hz shows that the 12 kHz dipolar width of the usual solid state spectrum has been eliminated. Figure 3a shows the result of a numerical simulation on a system of three dipolar coupled spins 1/2 with three distinct chemical shifts and confirms the effectiveness of the sequence even when both types of interactions are present.

With all internal magnetic interactions eliminated, the next step is to introduce an externally variable field in such a way that the line frequency does depend on it. In order for any such field to have a lowest-order effect on the rapidly toggling magnetization, it too must have a related time dependence. We avoid the technical difficulty of pulsing the DC field by instead modifying the rf field. Figures 1b) and d) show rf sequences which when superimposed on the sequences in a) and c), respectively, cause an apparent precession around the static field direction at a frequency proportional to their pulse angle θ. The experimental confirmation of this effect (superimposing the sequences of Fig. 1a) and 1b)) is shown in Fig. 2, where θ ranges from zero to 17 degrees with proportional changes in the line position. Fig. 3 shows the corresponding set of numerical simulations on the system with chemical shifts.

The significance of these results for NMR imaging of solids is that elimination of the dipolar and Zeeman interactions has been achieved in a sequence which gives a line position proportional to a continuously variable rf field strength. Figure 2 was obtained by combining the sequences of Fig. 1a) and b) in a single coil with a homogeneous field. If instead the sequence of Fig. 1b) were delivered by a rf coil whose field varied linearly across the sample, then the value of θ would label a particular

slice perpendicular to the gradient. The resulting spectrum would be the projection of the number density of the observed nuclear spin onto the gradient axis. The use of rf gradient coils in imaging of liquids has already been demonstrated.[20] Sequences like those of Fig. 1 should make the use of rf gradients the method of choice for imaging of solids. The advantage over sequences proposed[4] using pulsed DC gradients is a practical one; rf gradients of sufficient magnitude can be routinely switched in amplitude and direction in well under a microsecond.[20]. As a result of the high carrier frequency, the inductors can be small. Furthermore, they neither couple to the static gradient coils used to shim the field nor excite long-lived eddy currents, two effects which constrain the size and switching time of DC gradients.

The design process can be described using coherent averaging theory treating the pulses responsible for the precession (Fig. 1b) or 1d)) as a perturbation on the sequences of Fig. 1a) or 1c) in analogy to the standard treatment[13] of uncontrolled pulse angle errors. As an example, consider a nutation sequence consisting of pulses of angle θ_i coincident with the i^{th} pulse of Fig. 1a) and having the same phase. (More general timing and phases are possible, but will not be considered here for simplicity). The average Hamiltonian for this sequence of total length t_c is

$$\mathcal{H}^{(0)} = (1/t_c)(\kappa_y I_y + \kappa_z I_z) \qquad (1)$$

where $\kappa_y = (\theta_1 - \theta_4 - \theta_5 + \theta_8 - \theta_9 + \theta_{12} + \theta_{13} - \theta_{16})$ and
$\kappa_z = (\theta_2 + \theta_3 - \theta_6 - \theta_7 + \theta_{10} + \theta_{11} - \theta_{14} - \theta_{15})$.
Although resonance offset and chemical shift terms have been eliminated,

note that some of the pulse angles now appear as coefficients of the longitudinal component of spin angular momentum I_z. To obtain the sequence of Fig. 1b), these are set equal in magnitude ($|\theta_i| = \theta$) and their signs (i.e. phases) are chosen to maximize the magnitude of the coefficient of I_z. The result is an apparent resonance offset frequency of $8\theta/t_c$ radians/s. Effective transverse fields due to intentional pulse missets (analogous to the I_y term of Eq. (2)) have been used recently for spin locking[16].

The analysis of Eq. (1) suffices to explain the θ-dependent line positions in Figs. 2 and 3. To understand why such large angles can be treated perturbatively is more difficult. One approach is to calculate higher order correction terms $\mathcal{H}^{(n)}$[12-15] for the superimposed pulse sequence. The largest possible θ-dependent correction term is the cross-term between the nutation pulses and the dipolar couplings. As can be shown analytically, this term is zero for the sequences used. This is confirmed by the fact that the experimental linewidth in Fig. 2 increases only slightly with θ. No attempt has been made to calculate the algebraic form of the underlying correction term actually responsible for this weak θ dependence. It is of interest however, that the exact numerical simulation of Fig. 3, on a three spin system with dipolar couplings similar in size to those of adamantane, accurately reproduces the weak θ-dependent line broadening. This indicates the potential of such simulations as an adjunct to algebraic methods in evaluating new pulse sequences.

From the viewpoint of an imaging experiment, this line broadening represents a decrease in resolution towards the edges of the picture. Nevertheless, the resolution achieved suggests that images with $\gtrsim$50 picture elements in each spatial dimension are attainable. The other imperfection

is the small line at $\omega = 0$ in Fig. 2 even when $\theta \neq 0$. This corresponds to a bright spot at the center of the image and an effective degradation of the information content of that one picture element. This feature was not found in the numerical simulation of Fig. 3, which was performed with square pulses. One possibility is that it arises from the finite rise and fall time ($\sim 3 \times 10^{-7}$s) of the actual pulses.

An important requirement for sequences designed for high field imaging of protons is that they perform satisfactorily over the 10 ppm range of chemical shifts which characterize most solids. Results indistinguishable from Fig. 2 are found in a range of 2kHz about exact resonance indicating that an adequate bandwidth has been achieved.

The concept introduced here in one dimensional form will be most useful when incorporated into multidimensional experiments. Since the dynamics is reduced to that of a two level system with arbitrary linearly varying or spatially homogeneous coefficients for the transverse and longitudinal terms (Eq. (1)), imaging procedures such as "slice selection"[2] and Fourier zeugmatography[17], which were designed for liquids, are now possible in solids. The spatial information from the imaging dimension(s) may also be correlated with spectroscopic information by Fourier transforming with respect to an additional dimension where some part of the internal Hamiltonian is allowed to act in high field or zero field[21]. Such spectroscopic applications will allow the imaging of such properties as chemical identity, molecular structure, diffusion, restricted motion, reactivity, or spatial orientation. The improvement of these sequences and their incorporation into multidimensional imaging spectroscopy of solids is currently under way.

Acknowledgements

The authors thank Prof. A. Pines for his support and interest in this work. We also thank Gerry Chingas, Al Garroway, and Nick Szeverenyi for stimulating discussions of their work prior to publication. This work was supported by the Director, Office of Energy Research, Office of Basic Energy Sciences, Materials Science Division of the U.S. Department of Energy and by Director's Program Development Funds of the Lawrence Berkeley Laboratory under Contract Number DE-AC03-76SF00098.

References

1). P.C. Lauterbur, Nature 242, 190 (1973).

2). P. Mansfield and P.G. Morris, "NMR Imaging in Biomedicine" (Academic, New York, 1982).

3). P. Mansfield, P.K. Grannell, A.N. Garroway, and D.C. Stalker, Proc. 1st Spec. Colloque Ampere (J.W. Hennell, ed.) p. 16, Krakow, 1973.

4). P. Mansfield and P.K. Grannell, Phys. Rev. B 12, 3618 (1975).

5). R.A. Wind and C.S. Yannoni, J. Magn. Reson. 36, 269 (1979).

6). A.N. Garroway, J. Baum, M.G. Munowitz, and A. Pines, J. Magn. Reson. 60, 337 (1984).

7). N.M. Szeverenyi and G.E. Maciel, J. Magn. Reson. 60, 460 (1984).

8). B.H. Suits and D. White, Solid State Commun. 50, 291 (1984).

9). S. Emid and J.H.N. Creyghton, Physica 128B, 81 (1985).

10). G.C. Chingas, J.B. Miller, and A.N. Garroway, Abstracts of the 26th Experimental NMR Conference, Asilomar CA, 1985.

11). J.S. Waugh, L.M. Huber, and U. Haeberlen, Phys. Rev. Lett. 20, 180 (1968).

12). U. Haeberlen and J.S. Waugh, Phys. Rev. 175, 453 (1968).

13). W.K. Rhim, D.D. Elleman, L.B. Schreiber, and R.W. Vaughan, J. Chem. Phys. 60, 4595 (1974).

14). U. Haeberlen, "High Resolution NMR in Solids; Selective Averaging" (Academic, New York, 1976).

15). M. Mehring, "High Resolution NMR Spectroscopy in Solids" (Springer, Berlin, 1983).

16). L. Quiroga and J. Virlet, J. Chem. Phys. 81, 4774 (1984).

17). A. Kumar, D. Welti, and R.R. Ernst, J. Magn. Reson. 18, 69 (1975).

18). D.P. Weitekamp, J.R. Garbow and A. Pines, J. Chem. Phys. 77, 2870 (1982); J. Chem. Phys. 80, 1372 (1984).

19). D.P. Burum, M. Linder and R.R. Ernst, J. Magn. Reson. 44, 173 (1981).

20). D.I. Hoult, J. Magn. Reson. 33, 183 (1979).

21). D.P. Weitekamp, A. Bielecki, D. Zax, K. Zilm, and A. Pines, Phys. Rev. Lett. 50, 1807 (1983).

Figures

Figure 1: Nutation sequences for magnetic resonance imaging. The line narrowing cycle in a) eliminates evolution due to both the internal spin Hamiltonian and resonance offsets. The four quadrature rf phases are labeled x, y, $\bar{x}$, and $\bar{y}$. The pulse length is t_w and, as with the WHH-4 sequence (see Ref. 15, Sec. 3.5), the pulse angle $\beta_0 > \pi/2$ satisfies $\delta(1-\tan\beta_0/\beta_0) = 4/3$, where $\delta = 2t_w/(\tau_1 + \tau_2 + 2t_w)$. Optimal line narrowing is obtained with $(\tau_1 + t_w)/(\tau_2 + t_w) = 2.0$. Transverse magnetization is created by a $\pi/2$ pulse before the first such cycle and is sampled at the beginning of each cycle in a train. The sequence in b) runs concurrently with that in a) and forces a net precession of the magnetization through an angle 8θ where θ is the magnitude of the individual pulses in b). For NMR imaging, the sequence in b) is delivered by a rf field gradient coil, such that θ (and thus the rate of precession) varies linearly across the sample. The sequences in c) and d) form a similar pair. The 12-pulse windowless sequence of c) with length $t_c = 12t_w$ and pulse angle $\beta_0 = \pi/2$ narrows the line and its position is controlled by the angle θ in sequence d).

Figure 2: Experimental demonstration of line narrowing with nutation. The sequences of Fig. 1a) and b) were superimposed in a single coil by using pulse angles of $\beta_0 + \theta$ or $\beta_0 - \theta$ depending on whether the phase in b) is equal or opposite to that of the simultaneous pulse in a). The spectra shown are Fourier transforms of the resulting complex rotating frame signals. The variation from θ

= 0° in a) to θ = 17° in g) was obtained by varying pulse length around the value β_0 = 93° appropriate to the parameters t_w = 2.7μs, τ_1 = 10μs and τ_2 = 22.7μs. The linear variation in line position with θ confirms the analysis of Eq. (2). The effectiveness of line narrowing over the entire spectral width confirms the possibility of obtaining many resolved picture elements in an imaging experiment where frequency is proportional to spatial position in a gradient of θ. The absence of an image line at positive frequency shows that precession is confined to the transverse plane. Thus the imaging gradient may pass from negative to positive values within the sample without introducing any ambiguity with respect to signs.

Figure 3: Computer simulation of line narrowing with nutation on three coupled spins. The pulse timing and strengths are the same as in the corresponding traces of Fig. 2. For each value of θ, the evolution of the transverse magnetization was calculated for 500 repetitions of the sequences in Fig. 1a) and b) and then multiplied by an exponential decay corresponding to the experimental linewidth found for θ = 0 in Fig. 2a). The additional θ - dependent linewidth observed in Fig. 2 is also seen in the simulation indicating that it is intrinsic to the sequence and not due to experimental misadjustment. The dipolar couplings D_{12} = 3 kHz, D_{23} = 2 kHz and D_{31} = 1 kHz were chosen to give a spectral width similar to that of adamantane. Chemical shifts of ν_1 = -500 Hz, ν_2 = 100 Hz and ν_3 = 400 Hz

were added to demonstrate the effectiveness of the sequence in eliminating this source of spectral width.

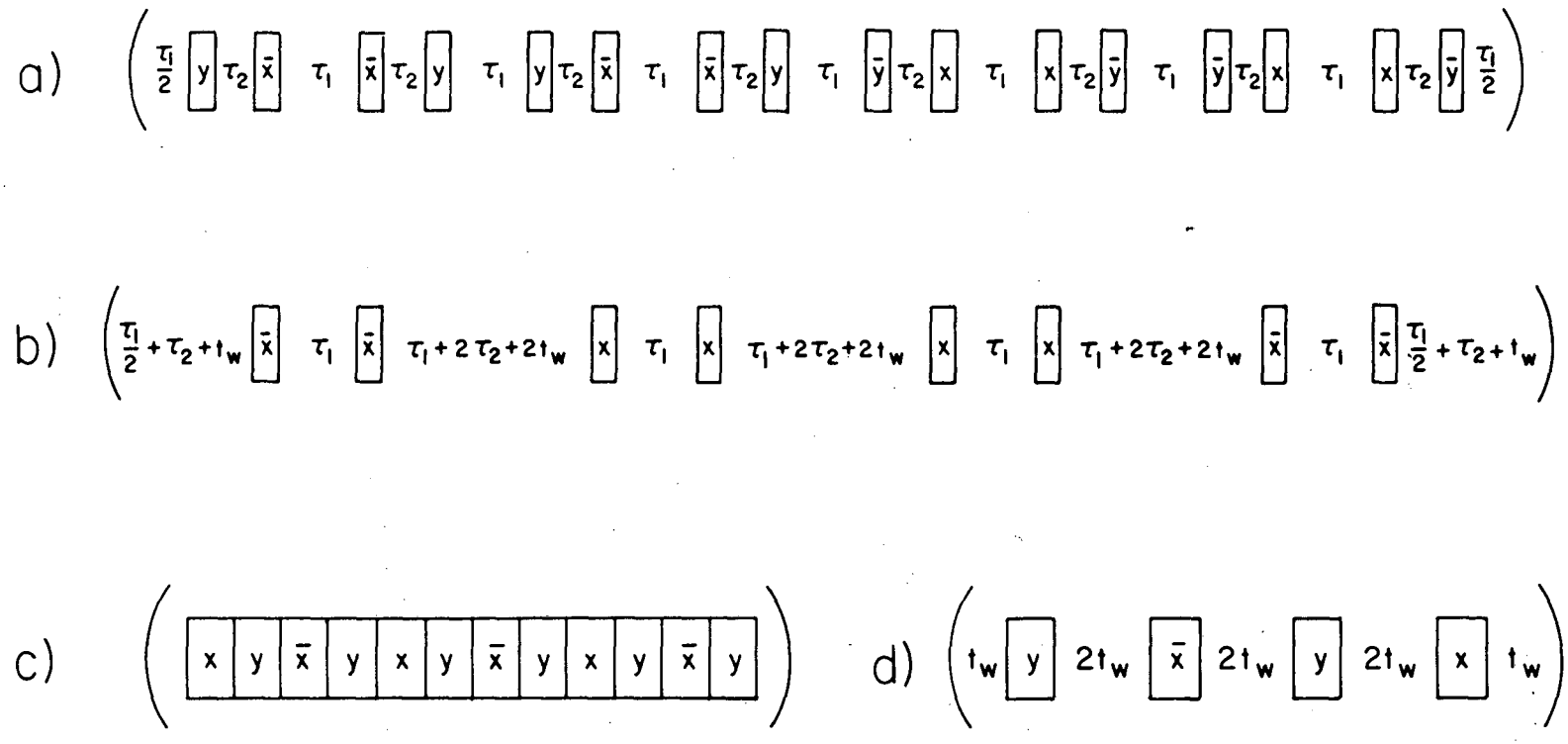

Figure 1

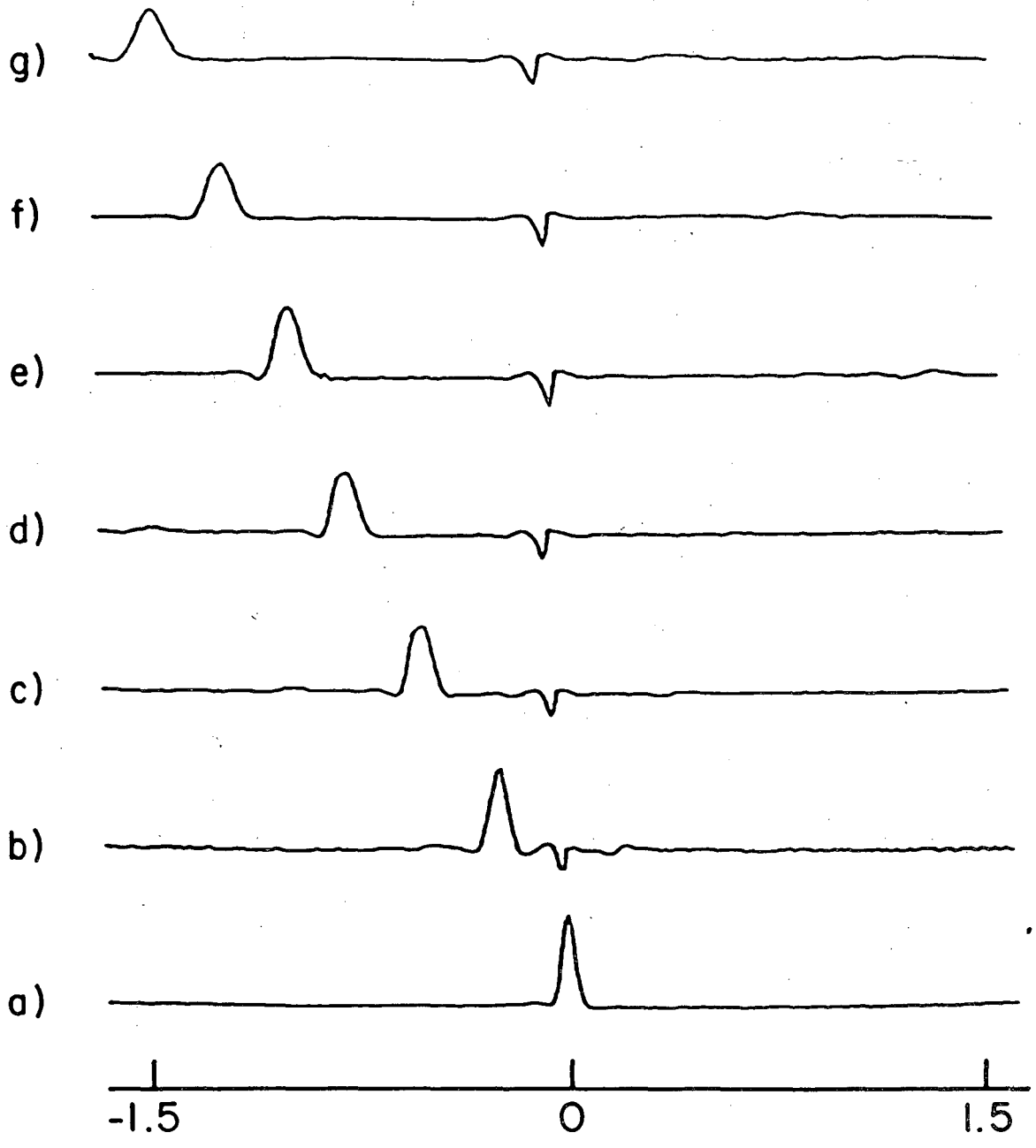

XBL 856-2892

Figure 2

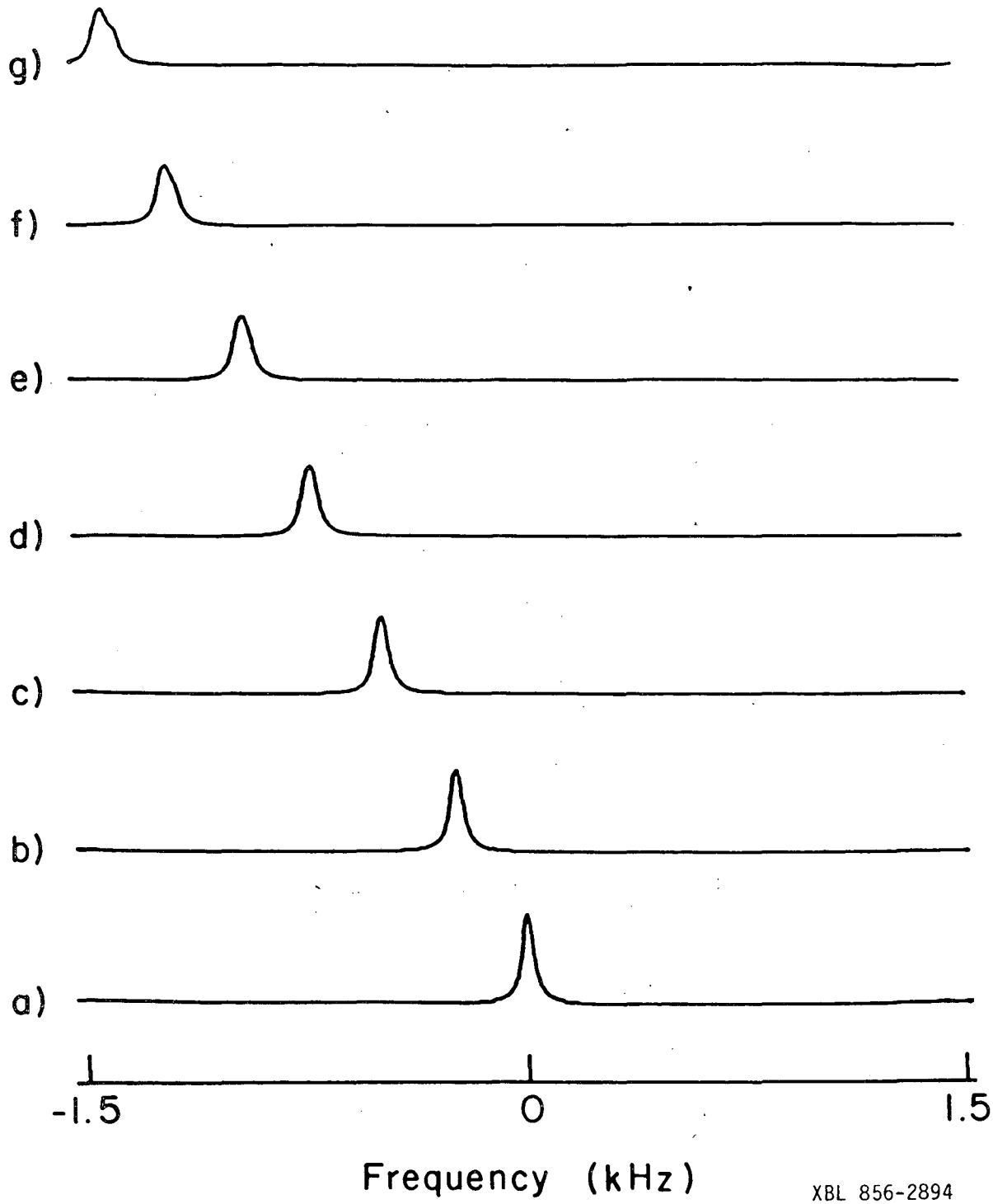

Figure 3

LAWRENCE BERKELEY LABORATORY
TECHNICAL INFORMATION DEPARTMENT
UNIVERSITY OF CALIFORNIA
BERKELEY, CALIFORNIA 94720